วิศวกรรมสารฉบับวิจัยและพัฒนา
Engineering Journal of Research and Development
วิศวกรรมสถานแห่งประเทศไทย ในพระบรมราชูปถัมภ์
The Engineering Institute of Thailand under H.M. The King's Patronage
ปีที่ 30 ฉบับที่ 2 เมษายน-มิถุนายน 2562
Volume 30 Issue 2 April-June 2019
Received 1 June 2018
Revised 9 July 2018
Accepted 19 July 2018
Physical Sciences

NUMERICAL INVESTIGATION OF AXIAL STRENGTH DEVELOPMENT IN METAL SHEET CONFINED CONCRETE

Tanyada Pannachet[1] and Maetee Boonpichetvong[2]
[1,2]Assistant Professor, Faculty of Engineering, Khon Kaen University, Khon Kaen 40002, Thailand.

ABSTRACT

This paper computationally investigated behavior of metal sheet confined concrete specimens subjected to axial compression. To understand mechanisms that occurred in the metal sheet confinement system during the loading, plain concrete specimens confined with 1-3 layers of metal sheet were analyzed via the three dimensional finite element analysis. Cylindrical and square cuboid concrete specimens of the same cross sectional area were selected to understand effect of specimen shapes on axial compression behavior of metal sheet confined specimens. The numerical results showed that the metal sheet confinement system could improve axial compression capacity of all the specimens. The improved stress-strain behavior of the specimens was not influenced by lateral confinement only, but also by ability of metal sheet in resisting axial compression. It was observed that shape and number of layers of confinement affected the strength increase. For two layers of metal sheet application, slightly different behaviors were found at the inner and the outer jackets. For the cuboid specimen, different behaviors at the region near the corner and on the side were noticed. The non-uniform stress distribution across the square section led to lower axial strength improvement when applying the same number of metal sheet layers, as compared to the circular section.

KEYWORDS: concrete, metal sheet, axial compression, finite element analysis, confinement.

บทคัดย่อ

บทความนี้เป็นการศึกษาพฤติกรรมของตัวอย่างคอนกรีตที่ถูกโอบรัดด้วยเมทัลชีท ตัวอย่างทดสอบในการศึกษาประกอบไปด้วยคอนกรีตล้วนและคอนกรีตที่ถูกโอบรัดด้วยเมทัลชีทจำนวน 1-3 ชั้น ใช้การจำลองโดยใช้วิธีไฟไนท์เอลิเมนต์แบบสามมิติ เพื่อให้ทราบถึงกลไกที่เกิดขึ้นในตัวอย่างระหว่างการรับน้ำหนัก ตัวอย่างคอนกรีตมีทั้งแบบทรงกระบอกและทรงสี่เหลี่ยมเพื่อศึกษาผลของรูปร่างของตัวอย่างคอนกรีตที่มีต่อพฤติกรรมการรับแรงตามแนวแกนด้วย จากผลการศึกษาพบว่า ระบบการเสริมกำลังนี้ช่วยเพิ่มความสามารถในการรับน้ำหนักตามแนวแกนของตัวอย่างได้ทุกตัวอย่าง โดยการเพิ่มกำลังไม่ได้มีผลจากการต้านทานด้านข้างเนื่องจากการโอบรัดเพียงอย่างเดียว แต่ยังมีผลจากการที่เมทัลชีทช่วยต้านทานแรงตามแนวแกนร่วมด้วย นอกจากนั้นยังพบว่ารูปร่างของตัวอย่างและจำนวนชั้นของการโอบรัดมีผลต่อการเพิ่มกำลังรับน้ำหนัก พฤติกรรมที่พบในเมทัลชีทจะมีความแตกต่างเพียงเล็กน้อยในเมทัลชีทชั้นในและชั้นนอกในกรณีที่โอบรัดด้วยเมทัลชีท 2 ชั้น สำหรับตัวอย่างทรงสี่เหลี่ยมพบว่า พฤติกรรมการรับแรงมีความแตกต่างกันที่บริเวณมุมและบริเวณกึ่งกลางด้าน การกระจายความเค้นที่ไม่สม่ำเสมอรอบรูปตัดของตัวอย่าง นี้ได้

ส่งผลให้ประสิทธิภาพการเพิ่มกำลังของตัวอย่างหน้าตัดสี่เหลี่ยมน้อยกว่าตัวอย่างหน้าตัดวงกลมที่ใช้จำนวนชั้นของเมทัลชีทที่เท่ากัน

คำสำคัญ: คอนกรีต, เมทัลชีท, แรงอัดตามแนวแกน, วิธีไฟไนท์เอลิเมนท์, การโอบรัด

1. Introduction

There are various techniques and various materials to externally strengthen structural members of buildings. One of the most popular choice is to use fiber-reinforced polymer (FRP) of various types as it possesses many advantages that make it suitable for external strengthening including its high strength, ease of installation, and high corrosion resistance. At present, there are vast collections of research focusing on applications of FRP in strengthening concrete columns, both experimentally [1-4] and numerically [5-9]. It was shown that the FRP confinement could increase axial compression capacity of concrete columns as well as their ductility [10, 11]. Many researchers found that level of strength improvement depended on various factors involving confinement efficiency, such as concrete strength, fiber properties, ply orientation, number of plies, thickness of the FRP, bond strength between the materials, shape and size of the column, and etc [12-19]. The stress-strain relationship of the confined column was found to be similar to the unconfined column during the earlier stage of loading [11, 13, 17]. However, when lateral expansion of the concrete core became larger, the FRP played an important role in resistance of the expansion, and thus higher axial strength could be obtained [13, 17].

While most of the recent research have been focused on development of the FRP strengthening system, other new techniques and materials are still in search. At our laboratory, we have been searching for alternative materials to the famous FRP for years. One of the possibilities is application of metal sheet, which are used widely in Thailand for roofing and architectural purposes. The metal sheet and the famous FRP contain some similar properties; both are thin and lightweight, therefore the material can be used externally to strengthen concrete members while conserving original architectural dimension of the building. Up to present, some preliminary laboratory experiments have been conducted on strengthening concrete members using metal sheet [20-23]. The experimental results revealed that the metal sheet jacketing was a possible alternative to the FRP jacketing in structural strengthening of concrete columns. It was found in [20] that axial capacity of concrete cylinders could be improved almost twice when confined with 3-layer G550 metal sheet of 0.23 mm thickness. Similar to the FRP, it was shown that the metal sheet confinement could upgrade the axial capacity as well as ductility of the columns. However, since the metal sheet jacket has rigidity along the axial direction, its behavior was found to be different from the FRP; it did not only restrain lateral expansion of the concrete core but also resist axial deformation together with the concrete core [21-24].

Knowledge about metal sheet as a strengthening material is still new to engineering community and has never been applied in engineering practice. Although existing experimental results have shown possibility of using the material for axial strengthening of concrete columns, there are still questions regarding how the metal sheet confinement system works in order to understand the behavior and to develop a proper design standard. Apart from the results from laboratory experiments, results from numerical modelling can provide some information that may not be visualized in the laboratory. So far, there have been some attempts of

numerical modelling to study behavior of the metal sheet confined concrete [25, 26]. However, those numerical studies were still limited to cylindrical specimens and did not provide sufficient information for the case of multiple layers of metal sheet application.

In this paper, we chose to investigate behavior of concrete specimens confined with metal sheet via three dimensional finite element analysis. Specimens with cylindrical and square cross sections were selected to study effect of the specimen shape on behavior of the confined concrete specimens. Results from the finite element analysis are presented and discussed.

2. Numerical experiments

In our numerical experiment, six specimens were modeled, three of which had circular cross sections (cylindrical specimens) and the other three had square cross sections (square cuboid specimens). Each of the sections comprised an unconfined specimen, a one-layer confined specimen, and a two-layer confined specimen. Cylindrical specimens and square cuboid specimens, both with 30-cm height, were of the size 15-cm diameter and 13.3-cm width, respectively. It was our purpose to fix the cross-sectional areas for both groups of specimens to be the same. Three dimensional modeling was considered. Since the specimens had some geometrical symmetries, one-eighth of the size was modeled instead of the whole specimen; only half the height and a quarter of the cross section were used. Geometrical models of the confined specimens are shown in Figure 1.

For the confined specimens, the finite element meshes consisted of three parts of material modeling; the concrete part, the adhesive part and the metal sheet part. Eight-node continuum brick elements, with 3 translational degrees of freedom per node were chosen for modeling the concrete and the metal sheet parts. To model the adhesive part, eight-node interface elements, with 3 degrees of freedom per node, were placed between the concrete and the metal sheet and also between layers of the metal sheet. For the unconfined specimens, only the concrete part was modeled. The $2 \times 2 \times 2$ Gauss quadrature rule was applied for each finite element.

Axial loading to the specimens was controlled by prescribing uniform vertical displacement at the top plane, whereas zero vertical displacement was specified at the bottom. On the planes of symmetry, displacements were restrained in the direction perpendicular to the plane, allowing symmetrical condition to be reserved.

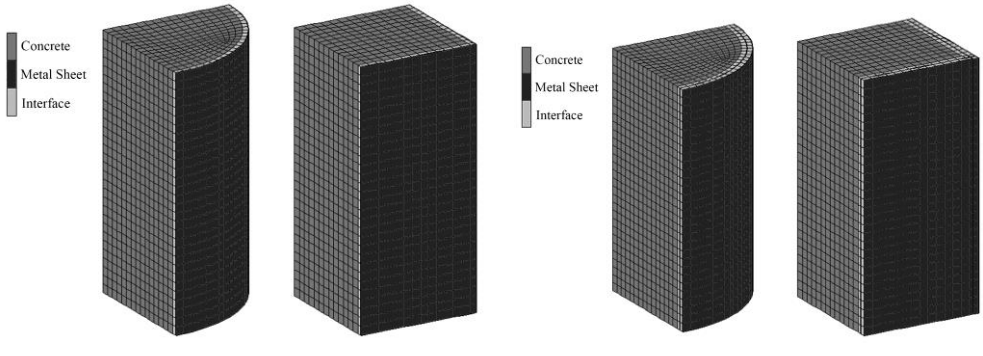

(a) One metal sheet layer (b) Two metal sheet layers

Figure 1 Finite element geometrical models for metal sheet confined concrete specimens.

3. Material modeling

As aforementioned, in modeling concrete columns confined with metal sheet, three materials were included. Details of each material model are given as follows.

3.1 Concrete modeling

The concrete part was considered as a homogeneous and isotropic material in this study. The mechanical properties used in the modeling of concrete are given in Table 1. In the nonlinear finite element modeling, stress-strain behavior of the concrete was based on Drucker-Prager yield criterion with associated flow rule, which is described as

$$F = \sqrt{J_2} + \alpha I_1 - \kappa \tag{1}$$

where I_1 is the first stress invariant or hydrostatic stress invariant,

$$I_1 = \sigma_1 + \sigma_2 + \sigma_3 \tag{2}$$

J_2 is the second deviatoric stress invariant,

$$J_2 = \frac{1}{6}\left[(\sigma_1 - \sigma_2)^2 + (\sigma_2 - \sigma_3)^2 + (\sigma_1 - \sigma_3)^2\right] \tag{3}$$

α is the frictional parameter and κ is the softening function defined as

$$\kappa = \left(1/\sqrt{3} - \alpha\right)\sigma_c \tag{4}$$

The frictional parameter α is based on the empirical formulation under triaxial compression. Using the confinement equation by Richart et al. [27], the frictional parameter α could be obtained as 0.2934 for use in this study. We used the softening function κ following Popovic's unconfined stress-strain relation [28],

$$\frac{f_c}{f_c'} = \frac{n\left(\frac{\varepsilon_c}{\varepsilon_{co}}\right)}{(n-1) + \left(\frac{\varepsilon_c}{\varepsilon_{co}}\right)^n} \tag{5}$$

where $n = 0.4\times10^{-3} f_c'[\text{psi}] + 1.0$ and ε_{co} is the strain in concrete at the peak stress (f_c') which is used as 0.002. To prevent mesh dependency problem usually found in the finite element analysis, our softening model for concrete was based on use of compressive fracture energy [29] defined as

$$G_{Fc} = \frac{A_{int}}{V_p} \tag{6}$$

where A_{int} is the area under the force-displacement curve until the displacement reaches 10% of the maximum load ($0.1P_{\max}$), and V_p is the localized fracture volume defined as volume of the finite element for this study.

The compressive fracture energy G_{Fc} depends on compressive strength of the concrete, but does not depend on shape and size of the specimen. For the normal strength concrete, the compressive fracture energy can be computed from

$$G_{Fc} = 0.86 \times 10^{-1} \left(f_c'\right)^{1/4} \quad \text{[MPa]} \tag{7}$$

Using the Drucker-Prager yield criterion results in an elastic-perfect plastic behavior of the material. When combining the yield criterion with the softening function, the obtained stress-strain behavior will be linear until reaching the elastic limit, after which it will be non-linear according to the specified softening function.

Table 1 Size of the specimens and the corresponding material properties used in the finite element modeling.

Material	Property	Value	Unit	Remarks
Concrete	Size	$\phi 15 \times 30$	[cm]	For circular section
		$13.3 \times 13.3 \times 30$	[cm]	For square section
	Compressive strength	22	[MPa]	
	Modulus of elasticity	22044.95	[MPa]	
	Poisson's ratio	0.20		
	Tensile strength	3.28	[MPa]	
Adhesive	Thickness of each layer	3	[mm]	
	Bonding strength	17	[MPa]	
	Modulus of elasticity	5000	[MPa]	
	Max elongation	0.4	%	
Metal sheet	Thickness of each layer	0.23	[mm]	
	Yield strength	550	[MPa]	
	Modulus of elasticity	200	[GPa]	
	Poisson's ratio	0.3		

In our model, behavior of concrete under tension was described using bi-linear softening function. Based on the smeared crack concept [30], cracking would occur in the direction perpendicular to the maximum principal tensile stress when the principal

tensile stress reached its maximum value. The softening behavior was modeled by using the fracture energy which is approximately 0.1 N/mm for concrete. The shear stress at the crack was analyzed by using the reduced shear modulus.

3.2 Metal sheet modeling

Since behavior of the metal sheet does not depend on the hydrostatic pressure, the Von-Mises yield criterion was chosen to model the elastic-perfect plastic material behavior of the metal sheet under tension and under compression. Properties of the metal sheet were taken from the manufacturer specification, as given in Table 1.

3.3 Adhesive (epoxy) modeling

The adhesive material was placed on interfaces between the concrete and the metal sheet, and between the metal sheet layers. To model delamination and slip at the interface, normal and shear stresses in each element were considered as bi-linear softening relations between the surface traction and the relative displacement (between the top and the bottom face), using properties given in the manufacturer specification, as given in Table 1.

4. Numerical results

4.1 Behavior of the cylinder confined with metal sheet

From the finite element analysis, the confined concrete cylinders showed an axial strength improvement from the plain concrete cylinder, depending on the number of metal sheet layers. For one-layer application, the axial stress was improved from 22.00 MPa to 28.17 MPa, making approximately 28% strength increase. For two-layer application, the axial strength was further improved to 35.69 MPa, which was approximately 62% more than the strength of the unconfined specimen. For three-layer application, the strength was 43.57 MPa, which was 98% improvement from the unconfined specimen.

In Figure 3, stress-strain relations of the one-layer and two-layer confined specimens were plotted. The graphs consisted of two parts; the right part showed axial stress - axial strain relation and the left part showed axial stress - lateral strain relation. Positive strain denoted strain in the compression, and negative strain presented strain in the tension. From Figure 3, the two sides of the graphs showed similar trends, i.e. the confined specimen provided higher axial load resistance in comparison to the unconfined specimen, considering at the same amount of axial or lateral deformation. Four critical points were marked in the confined specimen during the loading; Point A was where the concrete model reached the Drucker-Prager yield criterion, Point B was where the metal sheet reached the Von-Mises yield criterion, Point C was where the axial stress reached its maximum, and Point D was the end of the computation. For two-layer confinement, Point B could be indicated for the inner and the outer layers respectively as Point BI and Point BO, which were where the indicated layer of metal sheet yielded. When the plain concrete specimen was confined, there was an increase of hydrostatic pressure which consequently raised the yield stress of the specimen. Consider Point A of the three specimens, the yield stress was increased from 22 MPa for the unconfined specimen to 25 MPa for the one-layer confined specimen, and to 27 MPa for two-layer confined specimen. After the concrete yielding (cf. between Point

A and Point B), the specimen exhibited larger lateral expansion due to plasticity. The yielding occurred throughout the sheet due to uniform lateral expansion of the circular-shaped specimen. For two-layer confinement, the inner layer yielded first at Point BI, followed by the outer metal sheet layer which yielded at Point BO. Note that, in the post peak regime, the negative slopes were observed in the stress-strain relations of the unconfined and one-layer confined specimens. However, the slope became positive for the two-layer confined specimen.

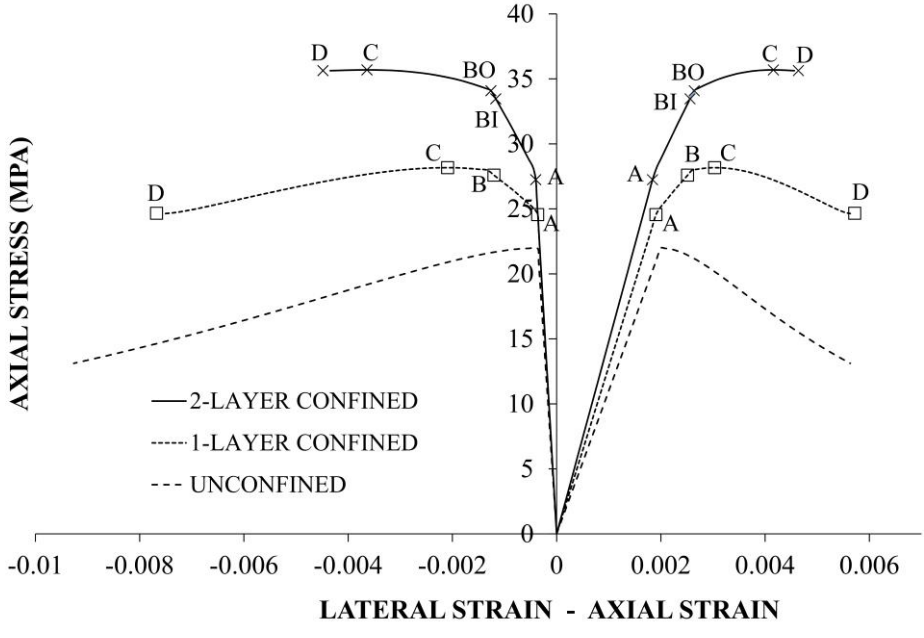

Figure 3 Stress-Strain relationship of the metal sheet confined concrete cylinder.

Figure 4(a) and Figure 4(b) show relationships between the axial stress and the axial strain, and between the circumferential stress (hoop stress) and the circumferential strain (hoop strain) in the metal sheet, respectively. In Figure 4(a), axial compressive stress was observed in the axial direction, implying that the metal sheet jacket took part in resisting axial loading along with the concrete core. In Figure 4(b), it was found that the circumferential stress showed compression at the beginning of the loading (before Point A). This could be due to difference of the Poisson's ratio between the metal sheet and the concrete core. Laterally, the concrete expanded less, thus restraining the metal sheet from free of expansion and leading to the compressive stress in the metal sheet. After Point A where the concrete yielded, the concrete core expanded much further due to plasticity. Tensile stress then arose in the metal sheet until it reached Von Mises yield criterion at Point B. After the metal sheet yielding, the concrete core still expanded laterally, causing higher tensile stress in the metal sheet. According to the elastic-perfect plastic material behavior specified in the metal sheet, when lateral stress was higher, it weakened ability to resist force in the other directions. Therefore, the axial compressive stress in the metal sheet became lower, as shown in Figure 4(a).

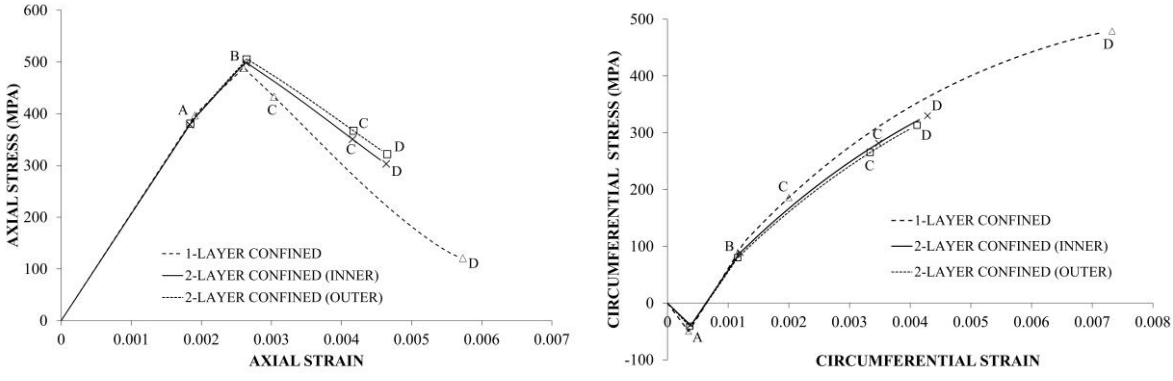

(a) (b)

Figure 4 Stress- strain relationship in the metal sheet of the confined concrete cylinders.

For two-layer confinement, behaviors found in the metal sheet were similar to those obtained in the specimen with one layer of metal sheet confinement. Only marginal differences between the inner and the outer metal sheet layers were observed. As sliding between the layers were allowed, the forces might not be fully transferred and therefore resulted in some marginally different behaviors between the two layers.

4.2 Behavior of the square cuboid confined with metal sheet

Similar to the cylindrical specimens, the finite element result showed that axial compressive strength of the concrete cuboids were improved by metal sheet confinement. When wrapping with one layer of metal sheet, the axial compressive strength of the square cuboid was improved from 22.00 MPa to 27.85 MPa, which was approximately 27% increase. With two and three layers of confinement, the strengths were improved to 32.94 MPa and 39.25 MPa, which were approximately 50% and 78% increase, respectively.

Behaviors of the one-layer and two-layer confined specimens are shown in Figure 6 in comparison to the behavior of the unconfined specimen. Five critical points in the curves were remarked; Point A was where the concrete started to yield, Point B was where middle of the side of the metal sheet started to yield, Point C was where corner of the metal sheet started to yield, Point D was where the specimen reached its maximum stress, and Point E was the end of the computation. Similar to what happened in the cylinder, confinement increased confining pressure in the concrete and slightly raised up the yield stress. After the yielding, the positive slope was still noticed from A to B before the metal sheet started to yield. The yielding started first at the middle of the side, where there was larger lateral expansion. Since the core concrete deformed less at the corner zone, yielding of the metal sheet at the corner zone occurred later at Point C. For two-layer confined cuboid, the metal sheet yielding took place at almost the same time for the outer and the inner layers, and it was the same point where the maximum stress was also obtained. After the specimen reached its maximum stress, softening behavior was observed for all the specimens.

The lateral strains shown in Figure 5 were measured at a point located at the middle of a side. The graphs would show different relationships if a different location was selected. In Figure 6, axial stress-lateral strain relations were plotted using the information at two different locations. For one–layer confinement, marginal difference of the lateral strains between two points were observed. However, for two-layer confinement, the lateral behavior near the corner apparently deviated from the behavior at the side. With higher level of confinement, the lateral expansion at the corner zone was more restrained, leading to a relatively more expansion at the side.

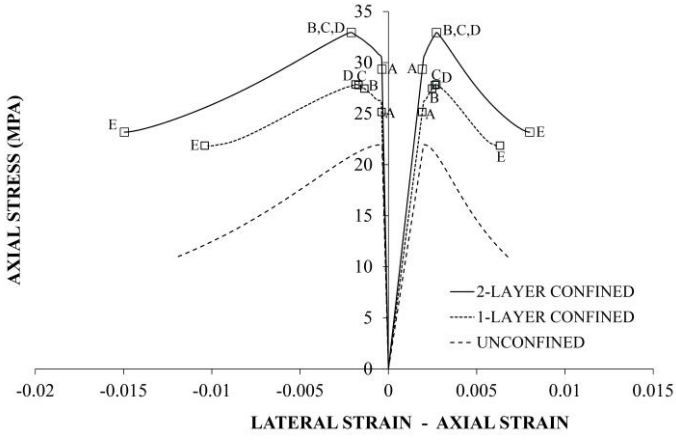

Figure 5 Stress-Strain relationship of the metal sheet confined concrete cuboids.

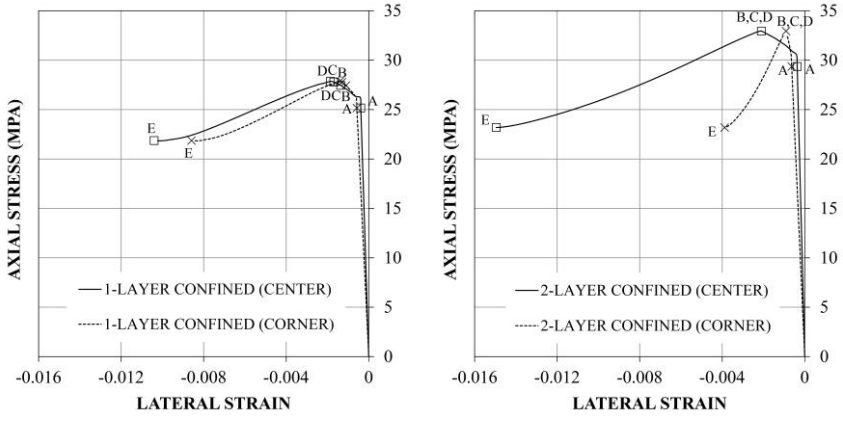

Figure 6 Axial stress-lateral strain relationship of the metal sheet confined concrete cuboid.

Due to restriction of the section shape, the square cuboid did not show uniform lateral expansion as in the cylinder. Due to non-uniform confinement, non-uniform distribution of stress and strain on the cross section was revealed. As shown in Figure 7, three zones were chosen, including Zone P the center of the specimen, Zone Q the side of the specimen and Zone R the corner of

the specimen. At the stage where concrete started to yield, the stress in the cross section was not uniformly distributed. The maximum stress occurred in Zone R which was the corner zone of the cuboid specimen. When the concrete core tried to expand laterally, it was restrained by the high sectional stiffness of the corner. Therefore, the confining stress acting on concrete around the corner became higher than the rest of the area. Correspondingly, the concrete in the corner zone yielded first and experienced higher equivalent plastic strain, followed by the rest of the cross section.

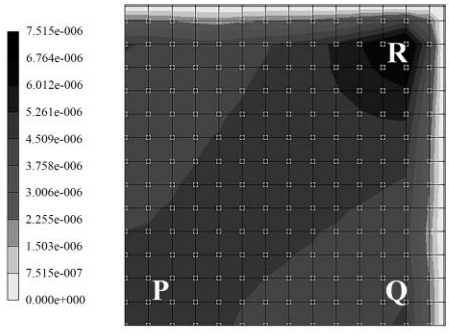

Figure 7 Equivalent plastic strain distribution at the concrete yielding of the one-layer metal sheet confined concrete cuboid.

4.3 Axial compressive strength increase

The axial compressive strengths of the confined concrete are summarized in Table 2 and plotted against number of layers in Figure 8. It can be seen that the axial strengths of the specimens were increased according to the number of applied layers in quite linear dependent trends. The section shape of the core specimen was an important factor to the amount of strength increase. Uniform confinement of the circular section specimens led to more efficiency in strength increase, as compared to the non-uniform confinement of the square section specimens. When confining the specimens with one layer of metal sheet, the strength increase in the cuboid was marginally smaller than in the cylinder of the same cross sectional area. However, more difference in the strength increase was noticed with more layers of metal sheet application, as shown in Figure 8.

Table 2 Axial compressive strength of the confined specimens.

Specimen	Number of layers	Axial compressive strength f_{cc} (MPa)	Normalized axial strength f_{cc}/f_{co}
Cylinder	1	28.17	1.28
	2	35.69	1.62
	3	43.57	1.98
Cuboid	1	27.85	1.27
	2	32.94	1.50
	3	39.25	1.78

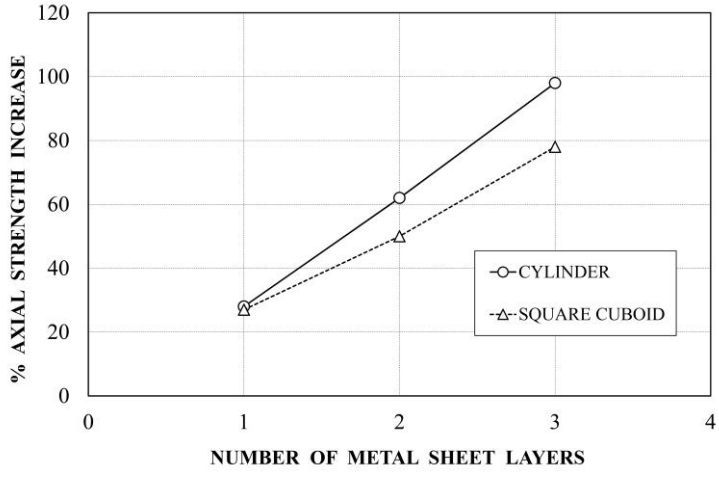

Figure 8 Effect of number of metal sheet layers on axial strength increase.

4.4 Verification of the finite element result

To verify the finite element models used in this study, the results obtained from the finite element analysis were compared with results from the laboratory experiments [23] and [24] for the cylindrical and square cuboid specimens of the same size, respectively (cf. Figure 9). Since the material properties from the laboratory experiment were different from the data used in our numerical test, normalization of the results was needed. Here, the normalized axial strength of the specimen (f_{cc}/f_{co}) was plotted against nf_y/f_{co} . Noted that f_{co} and f_{cc} are the axial strengths of unconfined and confined specimens, respectively, f_y is the yield stress of the metal sheet and n is number of applied metal sheet layers. It can be seen from Figure 10 that the result obtained from our numerical model could closely predict the axial compressive strength of the cuboid specimens from the laboratory.

Figure 9 The test specimens in the laboratory experiments [23-24].

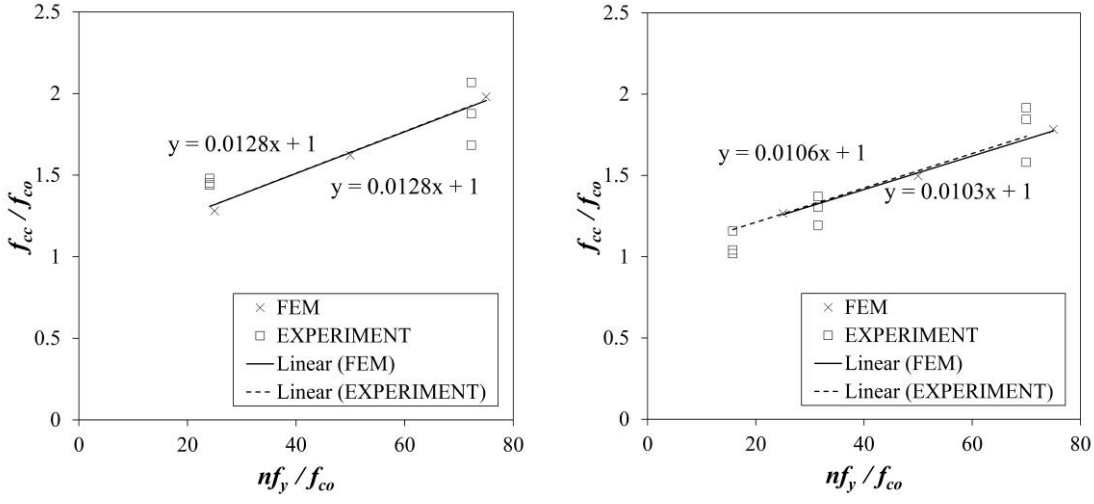

(a) Cylinder (b) Square cuboid

Figure 10 Comparison of the results obtained by the finite element analysis and the laboratory experiments.

5. Conclusions

The findings presented in this paper are summarized as follows:

1. The results from all the confined specimens revealed that the strengthening system could improve axial compression capacity of the original plain concrete specimens; higher axial strength increase could be obtained when applying more layers of metal sheet. Basically, the behavior of the confined system could be divided into two parts, i.e. before and after the yielding of concrete. It was found before the concrete yielded that the lateral expansion of the specimens, which depended on Poisson's ratio, was resisted by metal sheet confinement and resulted in higher yield stress as compared to the unconfined specimen. Stress distribution in the metal sheet also showed some resistance in the axial direction of the specimen, which could be seen together with the lateral resistance as a composite action.

2. Post peak behavior depended on number of applied metal sheet layers and also the cross section of the concrete core. For two-layer metal sheet confinement, slight hardening post peak behavior for the circular section specimens appeared, but not for the square section specimen. However, in all the square cuboid specimens, wrapping metal sheet up to two layers was still not sufficient to change the post peak behavior from softening to hardening. Axial compression behaviors of the confined specimens depended on the cross sectional shape of the core concrete.

3. Cross sectional shape of the specimens was one of the important factors in improving axial compression capacity of the specimens. For the circular cross section, the lateral expansion was uniform in the radial direction. The resulting confining pressure was uniformly distributed, providing high confinement effectiveness. On the other hand, for the square cross section, the lateral expansion was not uniform. More expansion was found at the side than the corner due to geometrical restriction. For the concrete core, higher stress was detected near the corner, which was the point the concrete yielded first. After the yielding, the metal sheet

at the side stretched more and thus restrained the metal sheet at the corner. This resulted in higher confining pressure induced in concrete at the corner of specimen.

4. Some of the finite element results were verified by comparison with existing experimental results, and found to be promising. The strength increases could be plotted in linear relations to the number of layers. Compared to the circular cross section, lower strength increase was obtained for the specimen with square cross section.

Acknowledgements

This research was supported by Sustainable Infrastructure Research and Development Center (SIRDC) and Faculty of Engineering, Khon Kaen University, Thailand.

References

[1] Teng, J.G., Chen, J.F., Smith, S.T., Lam, L. *FRP Strengthened RC Structures*. John Wiley & Sons Ltd, 2002.

[2] Shahawy, M., Mirmiran, A. and Beitelman, T. Tests and modeling of carbon-wrapped concrete columns. *Composites: Part B*, 2000, 31, pp. 471-480.

[3] Rochette, P. and Labossiere, P. Axial testing of rectangular column models confined with composites. *Journal of Composites for Construction (ASCE)*, 2000, 4(3), pp. 129-136.

[4] Parvin, A. and Brighton, D. FRP Composites strengthening of concrete columns under various loading conditions. *Polymers*, 2014, 6, pp. 1040-1056.

[5] Mirmiran, A., Zagers, K. and Yuan, W. Nonlinear finite element modeling of concrete confined by fiber composites. *Finite Elements in Analysis and Design* 2000, 35, pp. 79-96.

[6] Teng, J.G., Huang, Y.L., Lam, L. and Ye, L.P. Theoretical model for fiber-reinforced polymer-confined concrete. *Journal of Composites for Construction*, 2007, 11(2), pp. 201-210.

[7] Koksal, H.O., Doran, B. and Turgay, T. A practical approach for modeling FRP wrapped concrete columns. *Construction and Building Materials*, 2009, 23, pp. 1429–1437.

[8] Doran, B., Koksal, H.O. and Turgay, T. Nonlinear finite element modeling of rectangular/square concrete columns confined with FRP. *Materials and Design*, 2009, 30, pp. 3066–3075.

[9] Yu, T., Teng, J.G., Wong, Y.L. and Dong, S.L. Finite element modeling of confined concrete-I: Drucker-Prager type plasticity model. *Engineering Structures*, 2010, 32, pp. 665-679.

[10] Saatcioglu, M. and Razvi, S.R. Strength and ductility of confined concrete. *Journal of Structural Engineering (ASCE)*, 1992, 118(6), pp. 1590-1607.

[11] Wu, G., Lu, Z.T. and Wu, Z.S. Strength and ductility of concrete cylinders confined with FRP composites. *Construction and Building Materials*, 2006, 20, pp. 134-148.

[12] Mirmiran, A., Shahawy, M., Samaan, M. and Echary, H.E. Effect of column parameters on FRP-confined concrete. *Journal of Composites for Construction (ASCE)*, 1998, 2(4), pp. 175–185.

[13] Thériault, M., Neale, K.W. and Claude, S. Fiber-reinforced polymer-confined circular concrete columns: investigation of size and slenderness effects. *Journal of Composites for Construction (ASCE)*, 2004, 8(4), pp. 323-331.

[14] Yang, X., Wei, J., Nanni, A. and Dharani, L.R. Shape Effect on the Performance of Carbon Fiber Reinforced Polymer Wraps. *Journal of Composites for Construction (ASCE)*, 2004, 8(5), pp. 444-451.

[15] Almusallam, T.H. Behavior of normal and high-strength concrete cylinders confined with E-glass/epoxy composite laminates. *Composites: Part B*, 2007, 38, pp. 629-639.

[16] Al-Salloum, Y.A. Influence of edge sharpness on the strength of square concrete columns confined with FRP composite laminates. *Composites: Part B*, 2007, 38, pp. 640–650.

[17] Wang, L.M. and Wu, Y.F. Effect of corner radius on the performance of CFRP-confined square concrete columns: Test. *Engineering Structures*, 2008, 30, pp. 493–505.

[18] Wu, Y. and Wei, Y.Y. Effect of cross-sectional aspect ratio on the strength of CFRP-confined rectangular concrete columns. *Engineering Structures*, 2010, 32(1), pp. 32-45.

[19] Elsanadedy, H.M., Al-Salloum, Y.A., Alsayed, S.H. and Iqbal, R.A. Experimental and numerical investigation of size effects in FRP-wrapped concrete columns. *Construction and Building Materials,* 2012, 29, pp. 56–72.

[20] Saisaen, W., Damnernpol, H. and Ruangsak, A. *Compression strengthening of RC column by metal sheet*. Undergraduate Engineering Student Project Report, Khon Kaen University, Thailand, 2010. (In Thai)

[21] Pitakpupan, K., Groomrenthong, W. and Tongsuknork, Ch. *Confining mechanical behavior of metal sheet bonded around concrete column*. Undergraduate Engineering Student Project Report, Khon Kaen University, Thailand, 2010. (In Thai)

[22] Siramunin, G., Pila, Y. and Benjaprayunsak, W. *Effect of column sheet on failure mode of bonded metal sheet in strengthened columns*. Undergraduate Engineering Student Project Report, Khon Kaen University, Thailand, 2010. (In Thai)

[23] Khamthong, M., Boonpichetvong, M. and Pannachet, T. Axial compression strengthening of concrete columns confined by metal sheet. In: *Proceedings of the Seventh Annual Concrete Conference (ACC-7)*, Rayong, Thailand, October 2011. (In Thai)

[24] Boonyaratana, K., Pinitkarnwatkul, S. and Janpila, A. *Effect of concrete compressive strength on axial load carrying capacity of concrete column strengthened with metal sheets*. Undergraduate Engineering Student Project Report, Khon Kaen University, Thailand; 2012. (In Thai)

[25] Hongsinlark, N., Boonpichetvong, M. and Pannachet, T. Finite element modeling of axially loaded concrete columns with metal sheet confinement. *KKU Engineering Journal,* 2014, 41(4), pp. 517-525. (In Thai)

[26] Boonpichetvong, M., Pannachet, T. and Pinitkarnwatkul, S. Finite element modeling of concrete specimens confined with metal sheet strips. *International Journal of Technology,* 2016, 7, pp. 1132-1140.

[27] Richart, F.E., Brandtzaeg, A. and Brown, R.L. A study of the failure of concrete under combined compressive stresses. *Engineering Experimental Station Bull. No. 185,* Urbana, Illinois: University of Illinois, 1928.

[28] Popovics, S. A numerical approach to the complete stress strain curve for concrete. *Cement and concrete research*, 1973, 3(5), pp. 583-599.

[29] Lertsrisakulrat, T., Watanabe, K., Matsuo, M. and Niwa, J. Experimental study on parameters in localization of concrete subjected to compression. *Journal of Materials, Concrete Structures and Pavements (JSCE)*, 2001, 50, pp. 309-321.

[30] Rots, J.G. *Computational modeling of concrete fracture*. PhD Thesis, Delft University of Technology, Delft, the Netherlands, 1988.